DEVELOPMENTAL DYNAMICS 234:176–189, 2005

Localization and Loss-of-Function Implicates Ciliary Proteins in Early, Cytoplasmic Roles in Left-Right Asymmetry

Dayong Qiu, Shing-Ming Cheng, Laryssa Wozniak, Megan McSweeney, Emily Perrone, and Michael Levin*

Left-right asymmetry is a crucial feature of the vertebrate body plan. While much molecular detail of this patterning pathway has been uncovered, the embryonic mechanisms of the initiation of asymmetry, and their evolutionary conservation among species, are still not understood. A popular recent model based on data from mouse embryos suggests extracellular movement of determinants by ciliary motion at the gastrulating node as the initial step. An alternative model, driven by findings in the frog and chick embryo, focuses instead on cytoplasmic roles of motor proteins. To begin to test the latter hypothesis, we analyzed the very early embryonic localization of ciliary targets implicated in mouse LR asymmetry. Immunohistochemistry was performed on frog and chick embryos using antibodies that have (KIF3B, Polaris, Polycystin-2, acetylated α-tubulin) or have not (LRD, INV, detyrosinated α-tubulin) been shown to detect in frog embryos only the target that they detect in mammalian tissue. Immunohistochemistry revealed localization signals for all targets in the cytoplasm of cleavage-stage *Xenopus* embryos, and in the base of the primitive streak in chick embryos at streak initiation. Importantly, several left-right asymmetries were detected in both species, and the localization signals were dependent on microtubule and actin cytoskeletal organization. Moreover, loss-of-function experiments implicated very early intracellular microtubule-dependent motor protein function as an obligate aspect of oriented LR asymmetry in *Xenopus* embryos. These data are consistent with cytoplasmic roles for motor proteins in patterning the left-right axis that do not involve ciliary motion. *Developmental Dynamics 234:176–189, 2005.* © 2005 Wiley-Liss, Inc.

Key words: left-right asymmetry; cilia; motor protein; lrd; inversin; kif3b; polaris

Received 14 December 2004; Revised 17 May 2005; Accepted 20 May 2005

INTRODUCTION

The consistent left-right asymmetry of the heart, brain, and viscera of vertebrates raises fascinating questions about the evolutionary and embryonic origin of morphological handedness. While the downstream steps involving asymmetric gene expression are beginning to be characterized in molecular detail (Burdine and Schier, 2000; Yost, 2001; Levin, 2005), the initial steps of orienting the left-right axis are poorly understood. Important questions concerning the timing of the initiation of asymmetry and the conservation of mechanisms among different species remain open. Recently, a model (motivated by classical human data and functional experiments in mouse embryos) was proposed whereby embryonic asymmetry is generated by determinants moved extracellularly by the vortical motion of cilia in the node at gastrulation (Afzelius, 1999; Vogan and Tabin, 1999; Hirokawa, 2000a,b; Brueckner, 2001; McGrath and Brueckner, 2003; Tabin and Vogan, 2003). Molecular components relevant to this process and implicated in LR patterning include left-

Cytokine Biology Department, The Forsyth Institute, and Department of Oral and Developmental Biology, Harvard School of Dental Medicine, Boston, Massachusetts
Grant sponsor: American Cancer Society; Grant number: RSG-02-046-01; Grant sponsor: National Institute of Health; Grant number: 1-R01-GM-06227.
***Correspondence to: Michael Levin, Cytokine Biology Department, The Forsyth Institute, and Department of Oral and Developmental Biology, Harvard School of Dental Medicine, 140 The Fenway, Boston, MA 02115. E-mail: mlevin@forsyth.org**

DOI 10.1002/dvdy.20509
Published online 29 July 2005 in Wiley InterScience (www.interscience.wiley.com).

right dynein (LRD) (Supp et al., 1997, 1999a), Inversin (Yokoyama et al., 1993; Morgan et al., 1998), Polycystin-2 (Pennekamp et al., 2002), Kinesin-3B (Nonaka et al., 1998; Takeda et al., 1999), and Polaris (Murcia et al., 2000). This hypothesis is extremely attractive because it leverages morphological asymmetry from the biochemical chirality of cilia structure. A key component of this feature of the model is that the implicated proteins have their earliest LR-relevant roles in the node cilia at gastrulation.

However, the existing data are also compatible with a different model based on cytoplasmic functions of the motor proteins normally associated with ciliary motion (kinesin and dynein). We have previously proposed that asymmetric transport of LR determinants inside cells (presumably driven by the chirality of some cytoskeletal structure) is performed by these motor proteins long prior to gastrulation (Levin and Nascone, 1997; Levin and Mercola, 1998a); a related mechanism was also suggested by others based on the expression of *LRD* in mouse embryos (Supp et al., 1997). A detailed comparison of both models and the advantages and problems inherent in each are presented in Levin (2003, 2004a).

One specifically testable aspect of the intracellular transport model is its prediction that the ciliary targets, which have been functionally implicated in left-right asymmetry, should be expressed in embryos well before the appearance of cilia, and should exhibit localizations to cells and tissues unrelated to cilia function. This has been reported in mammals; for example, *lrd* is expressed in pre-streak mouse embryos (Supp et al., 1997). However, the localization of these targets has not been characterized in species in which very early LR patterning is best understood (e.g., *Xenopus*). Because the flat chick blastoderm is arguably a better model for understanding the fundamentals of axial patterning in mammalian (including human) development than the modified cylindrical topology of rodent embryos, inroads to understanding normal and pathological human laterality are likely to result from the characterization of early LR mechanisms in chick. Thus, we undertook to characterize and compare the localization of the implicated ciliary targets in both chick and *Xenopus* embryos, at stages earlier than those that had been examined in prior studies. Moreover, in contrast to gene expression analyses performed in a number of embryonic systems, we focused on protein localization. This is important because post-transcriptional mechanisms may establish asymmetries that would not be visible by characterization of mRNA localization, and because in *Xenopus* (and other systems) maternal proteins not dependent on the zygotic genome are likely to underlie important early phases of LR patterning.

In order to test the intracellular model of LR initiation, and to gain insight into possible novel cytoplasmic

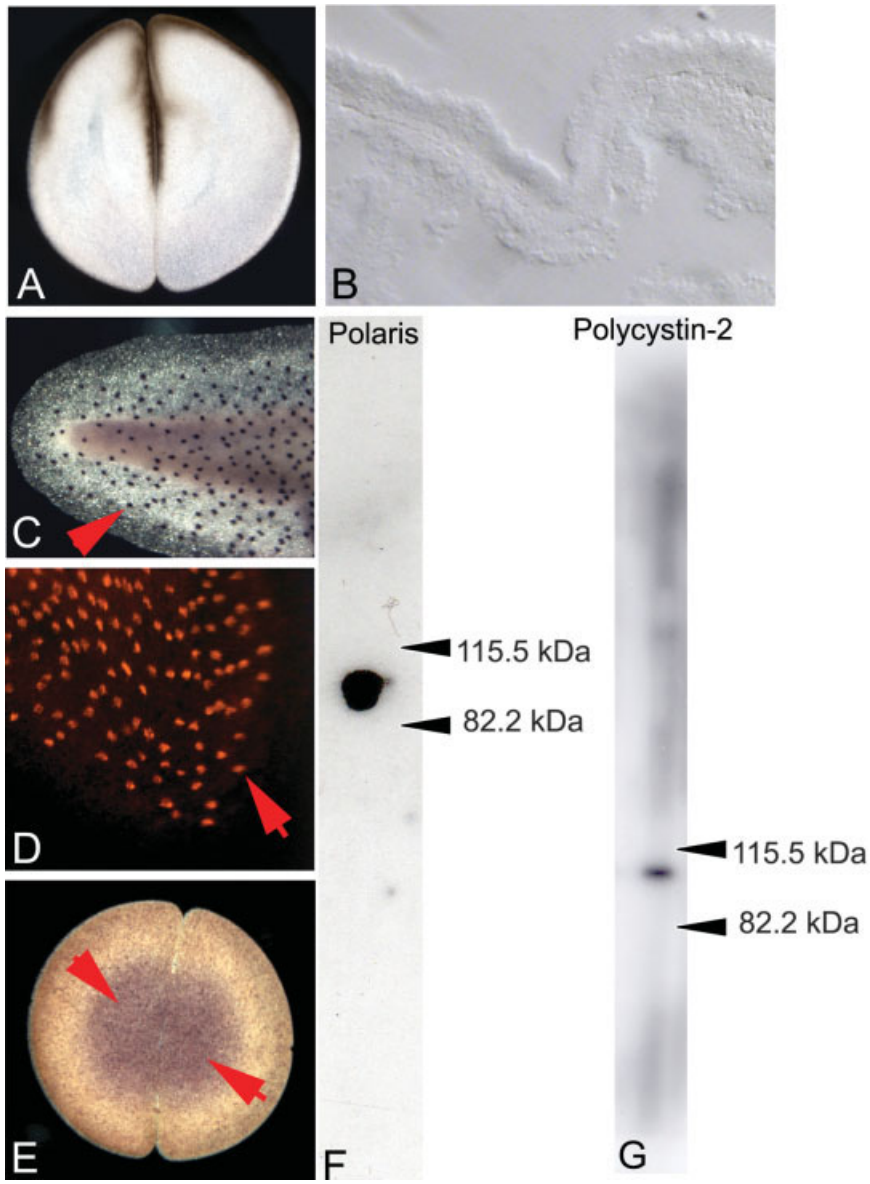

Fig. 1. Controls and antibody characterization. Sections processed for immunohistochemistry with no primary antibody, no secondary antibody, or with primary antibody pre-incubated with target peptide show no alkaline phosphatase signal in frog embryos (**A**, sectioned along the AV axis) or chick embryos (**B**, sectioned across the primitive streak at st. 3). As predicted, the inversin, LRD, and acetylated and detyrosinated α-tubulin antibodies correctly label cilia in older embryos (tail epidermis shown with alkaline phosphatase detection (**C**) or fluorescent secondary antibody, **D**). Most primary antibodies, such as Kinesin5 (**E**) reveal symmetrical stain in early embryos. In Western blots, the Polaris antibody reacts with a single band of the predicted size of 95 kDa (**F**), while the Polycystin-2 antibody reacts with a single band of the predicted size of 110 kDa (**G**). Red arrows, signal; white arrows, lack of signal; green arrows, additional signal.

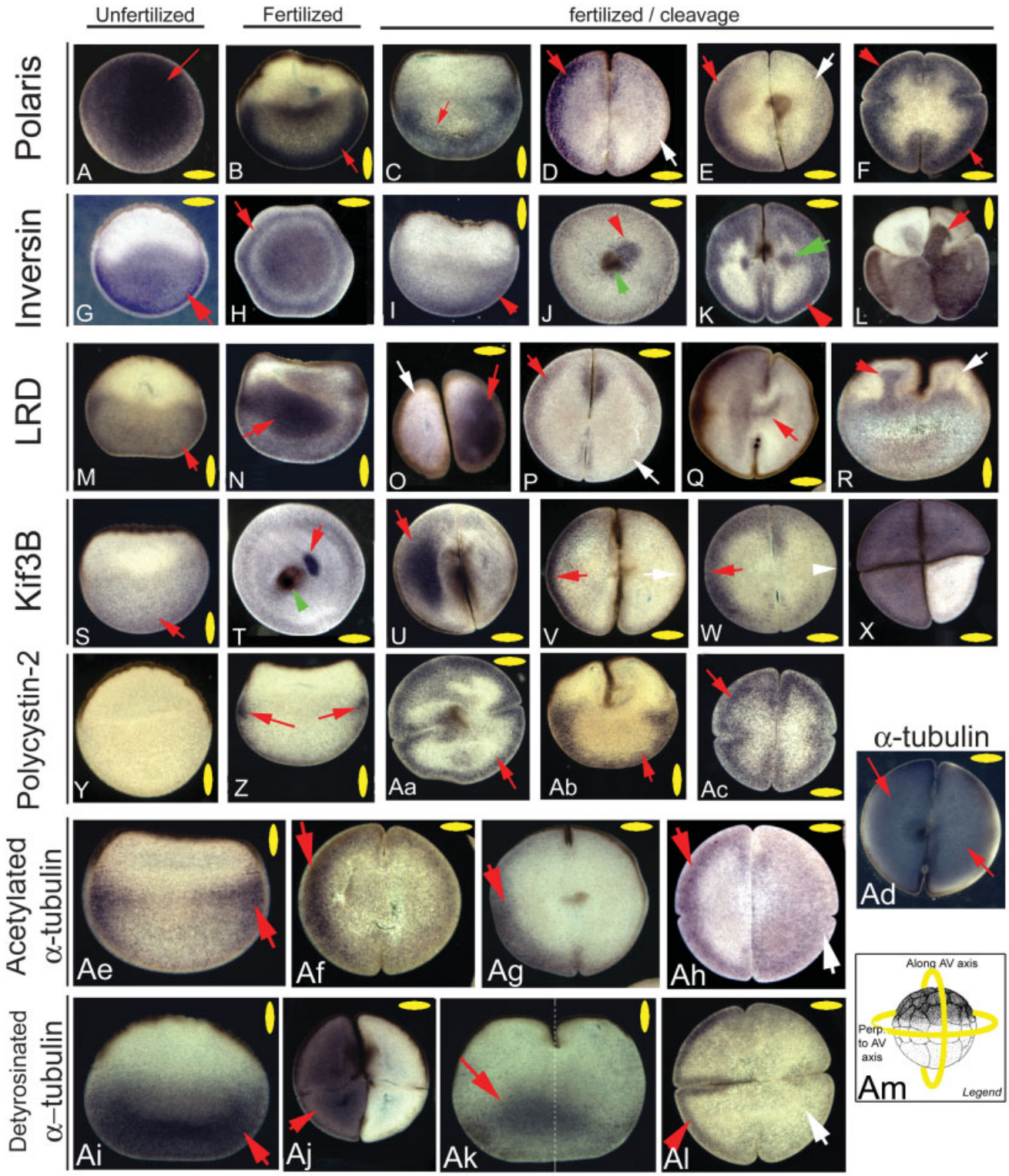

Fig. 2.

mechanisms of early LR patterning, we examined the localization patterns of key target proteins in two complementary model systems. We then performed loss-of-function experiments targeting cytoskeleton-directed motor transport. Taken together, our data obtained in two species with radically different gastrulation architectures demonstrate that all of the implicated targets are present in very early embryos, and suggest non-ciliary models of left-right asymmetry determination.

RESULTS

Analysis of Protein Localization in Early Embryos

For immunohistochemistry, frog embryos were fixed and sectioned in a gelatin-albumin block; this method utilizes an optically-transparent embedding medium, which is crucial for precise orientation of embryos prior to sectioning (Levin, 2004b). Additional advantages include avoiding tissue distortion (the medium serves as a scaffold but does not penetrate the tissue), high-temperatures, or organic solvents (embryos were processed at room-temperature, in aqueous solutions). Chick embryos were fixed, processed in wholemount, and then embedded and sectioned in JB4. An extensive series of controls was first performed. Frog (Fig. 1A) and chick (Fig. 1B) embryos undergoing immunohistochemistry without primary antibody, without secondary antibody, or with primary antibody pre-incubated with target peptide, resulted in a lack of signal. As predicted, Inversin, LRD, and the α-tubulin antibodies all labeled cilia in older embryos (Fig. 1C,D). In early embryos, most antibodies not implicated in asymmetry, such as other kinesins (Rodionov et al., 1991), are localized symmetrically in the cytoplasm (Fig. 1E).

We sought to examine the localization of several ciliary proteins of relevance to LR patterning. The antibodies to Kif3B (Le Bot et al., 1998; Ginkel and Wordeman, 2000) and acetylated α-tubulin (Sale et al., 1988; Dent and Klymkowsky, 1989; LeDizet and Piperno, 1991) have already been extensively characterized in *Xenopus* and are known to be specific for their targets. However, the other antibodies have only been used in mammals. We thus attempted to characterize them on frog embryo extracts. Antibodies to Polaris (Pazour et al., 2000) and Polycystin-2 (Arnould et al., 1999; Cai et al., 1999) recognized clean bands of the correct size, approximately 95 (Fig. 1F) and 110 kDa (Fig. 1G), respectively, illustrating the conservation of their specificity to frog cells. Despite repeated attempts, the antibodies to LRD and Inversin did not work well in Western blots.

We utilized a total of seven antibodies in immunohistochemistry on a representative series of early stages in both species. Positive signal was blue (resulting from the alkaline phosphatase-conjugated secondary antibody). The expression patterns shown in Figures 2 and 3 represent the consensus analysis of at least 5 separate rounds of immunohistochemistry (although there was some variability among embryos and among sections taken at different levels within an embryo). All targets were detected in the cytoplasm as maternal proteins from the earliest stages in *Xenopus,* and in the base of the primitive streak in the chick (long prior to the appearance of a node and ciliated cells therein).

Localization of Ciliary Proteins in Frog Embryos

Polaris is the protein product of the mouse *Tg737* gene; mutations in this locus result in defects of midline development, preaxial polydactyly, and randomization of *situs* (Murcia et al., 2000). In mouse embryos, *Tg737* is expressed by day 6.5, although cleavage stages do not appear to have been ex-

Fig. 2. Localization of targets in unperturbed frog embryos. Polaris: (**A**) section taken perpendicular to the AV axis in the unfertilized *Xenopus* egg; (**B**) section taken parallel to the AV axis in an unfertilized egg; (**C**) section taken parallel to the AV axis in the fertilized egg; (**D**) in sections taken perpendicular to the AV axis in the 2-cell embryo, one of the two blastomeres shows strong stain near the cell membrane, although the other blastomere occasionally has some stain as well (**E**). In the 4-cell embryo, all four blastomeres exhibit cell membrane stain (**F**). Inversin: (**G**) section taken along the AV axis in the unfertilized egg; (**H**) section taken perpendicular to the AV axis in the unfertilized egg; (**I**) signal is seen in the vegetal cortex in fertilized eggs sectioned parallel to the AV axis, and can be detected in the microtubule organizing center (**J**; brown stain indicated by the green arrow is pigment brought in by the sperm entry trail); (**K**) section taken perpendicular to the AV axis at the 4-cell stage; (**L**) section taken along the AV axis at the 8-cell stage, animal pole is upwards. LRD: (**M**) section taken along the AV axis of the unfertilized egg; (**N**) section taken along the AV axis of a fertilized egg; (**O**) section perpendicular to the AV axis taken close to the animal pole reveals staining throughout one of the two blastomeres. **P**: sections taken through the equator perpendicular to the AV axis show asymmetric staining near the membrane cortex; (**Q**) some sections taken perpendicular to the AV axis revealed staining between the blastomeres before the completion of the cleavage furrow; (**R**) sections parallel to the AV axis reveal a rod of signal from the vegetal pole towards the animal pole, in one of the two blastomeres. KIF3B: (**S**) section along the AV axis of the unfertilized egg; (**T**) sectioning perpendicular to the AV axis of the fertilized egg reveals staining in the MTOC at nuclear fusion (brown stain is pigment brought in by the sperm entry trail, green arrowhead). Two-cell embryos sectioned perpendicular to the AV axis exhibit signal in the center (**U**) or in the membrane cortex (**V,W**) of one blastomere; (**X**) sections taken perpendicular to the AV axis at the four-cell stage reveal that staining is often absent from one of the four blastomeres on the right side. Polycystin-2: (**Y**) sections taken along the AV axis of the unfertilized egg show no signal; (**Z**) section of fertilized egg taken parallel the AV axis; (**Aa**) section taken perpendicular to the AV axis at the 2-cell stage; (**Ab**) section taken parallel to the AV axis at the 2-cell stage; (**Ac**) section taken across the AV axis at the 4-cell stage. α-tubulin: (**Ad**) antibodies recognizing all tubulin subunits stain throughout the cytoplasm of sections taken across the AV axis of the 2-cell embryo. Acetylated α-tubulin: (**Ae**) sections of fertilized and unfertilized eggs along the AV axis revealed spots of signal at the equator; (**Af**) sections of 2-cell embryos taken perpendicular to the AV axis revealed signal at the membrane cortex in one of two blastomeres; (**Ag**) section taken near the animal pole, across the AV axis of the 4-cell embryo. **Ah**: section taken near the vegetal pole, across the AV axis of the 4-cell embryo. Detyrosinated α-tubulin: (**Ai**) section of an unfertilized egg along the AV axis; (**Aj**) section taken across the AV axis of embryos at the 4-cell stage; (**Ak**) sections taken parallel to the AV axis at the 2 cell stage (dashed line indicates embryonic midline); (**Al**) section taken across the AV axis of a 4-cell embryo. **Am:** In each panel, yellow ovals with their long axis oriented left to right indicate that the section was taken across the AV axis; yellow ovals with their long axes oriented vertically indicate that the section was taken along the AV axis, with the animal pole being upward. Red arrows, signal; white arrows, lack of signal; green arrows, additional signal.

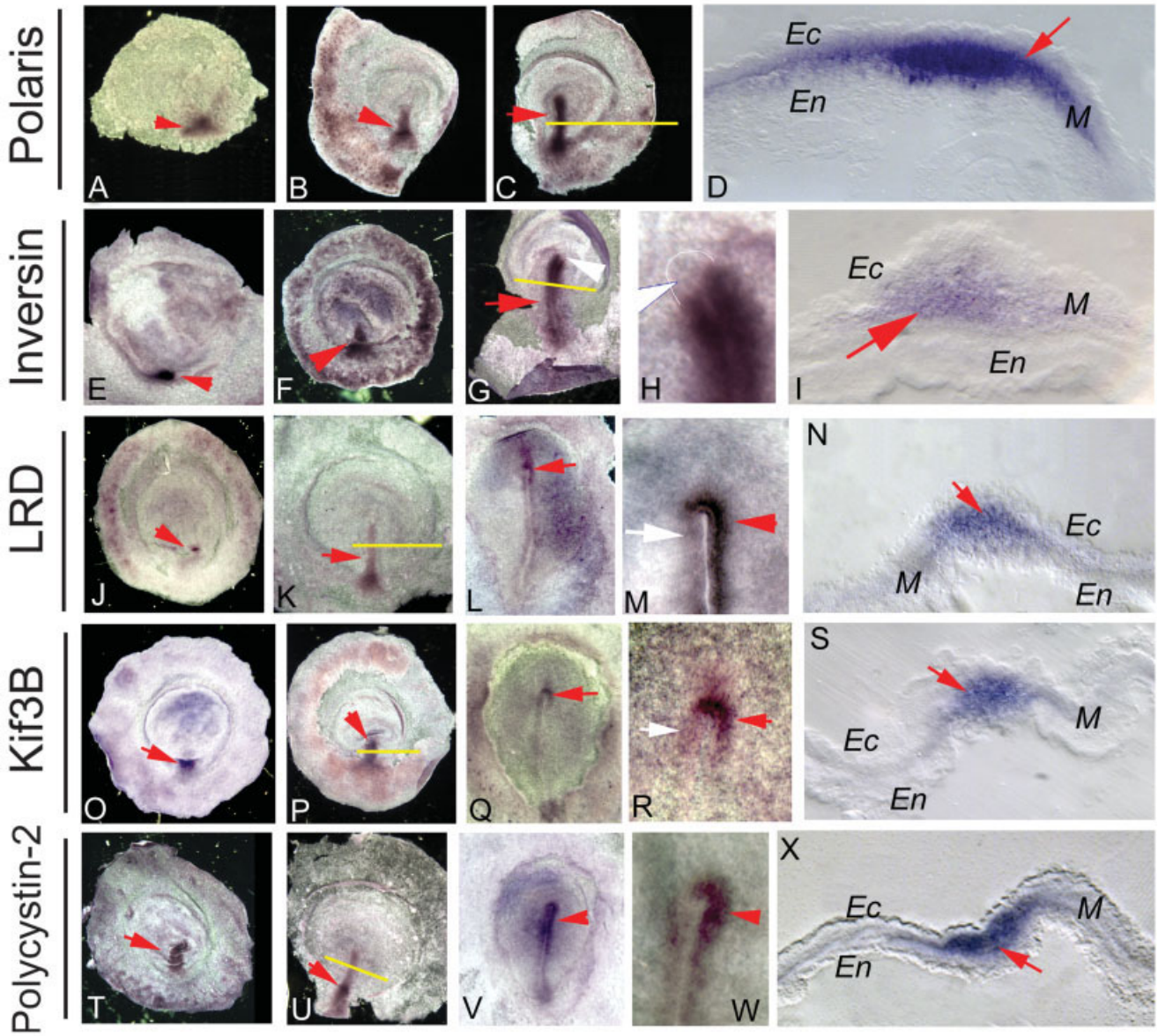

Fig. 3. Localization of targets in unperturbed chick embryos. Yellow line in each panel indicates plane of section. In each section panel, Ec = ectoderm, En = endoderm, M = mesoderm. Polaris: (**A**) 6-hr chick embryo; (**B**) st. 2 embryo; (**C**) st. 3 embryo; (**D**) section taken through a st. 3^- embryo. Inversin: (**E**) 6-hr chick embryo; (**F**) st. 1 embryo; (**G**) st. 3^+ embryo; (**H**) close-up of anterior tip of the streak at st. 3^+; (**I**) section taken through the streak at st. 2. LRD: (**J**) st. 1 chick embryo; (**K**) st. 2 embryo; (**L**) st. 4^+ embryo; (**M**) close-up of node at st. 4; (**N**) section taken through the streak at st. 2. KIF3B: (**O**) st. 1 chick embryo; (**P**) st. 2 embryo; (**Q**) st. 4^+ embryo; (**R**) close-up of node at st. 4; (**S**) section taken through the streak at st. 2. Polycystin-2: (**T**) st. 2 embryo; (**U**) st. 3 embryo; (**V**) st. 4 embryo; (**W**) close-up of node at st. 4; (**X**) section taken through the streak at st. 3. Red arrows, signal; white arrows, lack of signal; green arrows, additional signal.

amined yet. Polaris localizes to cilia (Taulman et al., 2001), as well as basal bodies, whose 3-dimensional chirality is an ideal candidate for an "F-molecule" which nucleates cytoskeletal tracks (Brown and Wolpert, 1990; Levin and Mercola, 1998a). In the frog embryo, Polaris is present in a radially symmetrical band around the vegetal pole of the egg before and after fertilization (Fig. 2A–C). The 2-cell embryo exhibits symmetrical Polaris localization throughout the vegetal half of the embryo; strikingly, embryos exhibit asymmetrical Polaris signal in one cell in sections taken near the animal pole (Fig. 2D,E). By the second cell cleavage, localization is symmetrical, near the cell membrane of all four blastomeres (Fig. 2F).

Mutation of *Inversin*, a protein with highly conserved ankyrin repeats, results in almost full LR reversal in mice (Mochizuki et al., 1998); it is expressed in mouse embryos from the 2-cell stage (Eley et al., 2004), but its function has not been elucidated. Besides its localization to cilia in some cells, Inversin interacts directly with tubulin and N-cadherin in the cytoplasm (Nurnberger et al., 2002) and it is known to localize to cell:cell junctions, plasma membrane, and polarized microtubule pools within cells (Nurnberger et al., 2002, 2004; Eley et al., 2004). In unfertilized frog eggs

and fertilized eggs prior to first cleavage, Inversin signal was observed in a radially-symmetrical pattern in the vegetal hemisphere (Fig. 2G–I), and is also localized to a spot adjacent to the sperm pronucleus (Fig. 2J). In two-cell embryos, Inversin is localized to the cell membrane (Fig. 3K, red arrowhead). Consistent with the 2 putative nuclear localization sequences (Morgan et al., 2002), Inversin signal was detected in a discrete spot within the cytoplasm (Fig. 2K, green arrow). In 8-cell embryos, Inversin protein is spread throughout the vegetal blastomeres, but extends in a rod-like pattern into the animal pole cells. The localization is significantly stronger on the right side (Fig. 2L).

LRD (Supp et al., 1997) is a dynein heavy chain gene identified as the locus of the murine *iv* mutation, which unbiases laterality (Lowe et al., 1996). It is expressed in cells of the mouse node (Supp et al., 1997) but also in blastocyst (day 3.5) cells; a striking antisymmetry in expression during head-fold stages has also been reported (Supp et al., 1999b). Expression of *LRD* was recently examined in a variety of species including chick and *Xenopus* (Essner et al., 2002); however, that study did not include data on protein localization or expression at pre-gastrulation stages. In *Xenopus* embryos, LRD was detected in a diffuse pattern in the vegetal half of eggs (Fig. 2M). Immediately after fertilization, LRD coalesced to a centralized spot in the center of the embryo (Fig. 2N). In two-cell embryos, a striking asymmetry was observed: stain was localized throughout only one of the two blastomeres in perpendicular sections taken near the animal pole (Fig. 2O). In sections taken through the equator, asymmetric stain near the membrane cortex was observed; stain was also seen at the cleavage furrow on both sides (Fig. 2P). In some sections before the cleavage furrow was complete, signal was observed in more complex patterns consistent with movement between blastomeres (Fig. 2Q, red arrowhead). Sections taken parallel to the animal-vegetal (AV) axis at the 2-cell stage reveal diffuse staining in the vegetal pole, and a specific shaft or finger-like projection towards the animal pole. In many embryos, this was observed in only one blastomere (Fig. 2R); this asymmetry continued in 8-cell embryos.

Kinesin 3B (KIF3B) is a member of a family of microtubule-dependent kinesin motor proteins; genetic deletions in this gene result in randomization of the *situs* of the viscera in mice (Nonaka et al., 1998). However, expression in embryos younger than day 7 has not been characterized. In unfertilized frog embryos, KIF3B is localized diffusely within the vegetal pole of cells (Fig. 2S). Immediately after fertilization, KIF3B is localized within the microtubule-organizing center (Fig. 2T). During the first two cleavages, KIF3B exhibits a very dynamic pattern among embryos of slightly different age. It can be detected in one of two cells within the cytoplasm (Fig. 2U), at the cell membrane of just one of the blastomeres near the animal pole (Fig. 2V,W), or throughout the cytoplasm of three out of four blastomeres after the second cell cleavage (Fig. 2X).

A recent analysis of the PCKD (polycystic kidney disease) mouse model found LR defects in animals carrying a targeted deletion of the ion channel Polycystin-2 (Pennekamp et al., 2002). Polycystin-2 appears to form a cation channel (Vassilev et al., 2001; Koulen et al., 2002), which can be expressed on the cell membrane (Hanaoka et al., 2000) and is transcribed in mouse embryos from the 2-cell stage (Pennekamp et al., 2002). Our localization data were identical using the N- or C-terminal antibodies (Pazour et al., 2002). In unfertilized *Xenopus* embryos, no Polycystin-2 signal was detected (Fig. 2Y). Shortly after fertilization, spots of Polycystin-2 localization were observed at the equator (Fig. 2Z). By cleavage stages, Polycystin-2 was symmetrically-expressed at the cell membrane (Fig. 2Aa–Ac), consistent with a proposed role as an ion channel.

Characterization of Microtubule Sub-Populations in Frog Embryos

The numerous mouse mutants that possess both cilia defects and LR asymmetry phenotypes (Afzelius, 1999; McGrath and Brueckner, 2003) suggest that a fundamental link may exist between mechanisms that control ciliary structure and asymmetry. Moreover, the *Xenopus* data presented above suggest the question: why would proteins normally associated with cilia be specifically localized inside the cytoplasm of early embryonic cells, and, if they were, what would control their spatial distribution? Work in a number of other species indicated that stable subpopulations of microtubules distinguished by acetylation and detyrosination proportional to their age (Maruta et al., 1986; Webster et al., 1990) exist in various cell types and appear to be associated with intracellular movement of both kinesin and dynein (Nilsson et al., 1996; Harrison and Huebner, 1997). Thus, we next asked whether the cytoplasm of early *Xenopus* embryos might contain microtubule populations carrying these modifications (indicative of less-dynamic structures) and thus regulating the localization of ciliary proteins inside the cell analogous to their presence inside cilia and flagella.

We used antibodies to two well-characterized ciliary markers: detyrosinated α-tubulin - ID5 (Wheatley et al., 1994) and acetylated α-tubulin (LeDizet and Piperno, 1991). To ensure that any observed signal was not reflective of simple concentration differences of total α-tubulin, we probed early embryos with an antibody that detects all α-tubulin (LeDizet and Piperno, 1991; Morales and Fifkova, 1991), which revealed the expected ubiquitous and symmetrical signal throughout the cells (Fig. 2Ad). We observed that in early frog embryos, acetylated tubulin was localized in a crescent around the animal pole of unfertilized eggs (Fig. 2Ae). Strikingly, during cleavage stages, asymmetric (one-sided) localization of acetylated tubulin was detected at the membrane cortex in one of two blastomeres (Fig. 2Af, Ag). At the 4-cell stage, asymmetric expression was present in the left blastomeres (Fig. 2Ah). Detyrosinated tubulin antibody stain was detected throughout the vegetal pole of unfertilized eggs (Fig. 2Ai), but much heavier localization was detected in the left blastomeres at the 4-cell stage (Fig. 2Aj, Ak). At the 4-cell stage, similarly to acetylated tubulin, detyrosinated tubulin was localized to

the cortex under the cell membrane of the left blastomeres (Fig. 2Al).

Localization of Ciliary Proteins in Chick Embryos

To investigate the evolutionary conservation of possible early roles for ciliary proteins, we next examined the localization of these targets in the early chick embryo. Polaris is strongly expressed at the origin of the primitive streak and continues to be present in the primitive streak throughout elongation (Fig. 3A–C). Polaris-expressing cells are in the mesoderm layer of st. 3 embryos (Fig. 3D). Inversin exhibits a low level of background expression in many cells of the area opaca before st. 2, but is particularly strongly expressed at the base of the streak during initiation (Fig. 3E) and throughout the streak during elongation (Fig. 3F,G). By st. 3^-, the background expression outside of the streak is significantly reduced (Fig. 3G). At st. 4, it is specifically absent from the most anterior part of Hensen's node (Fig. 3H, white arrowhead). Sectioning reveals that Inversin-containing cells are mesodermal (Fig. 3I). LRD was not detected in unincubated eggs, but became specifically expressed at the origin of the primitive streak (Fig. 3J). It was lightly and symmetrically expressed throughout the primitive streak during elongation (Fig. 3K). At st. 4^+, a right-sided localization was observed in Hensen's node (Fig. 3L, close-up in Fig. 3M). Sectioning revealed that LRD protein was located in the mesodermal cell layer in the early streak (Fig. 3N).

KIF3B was first detected at the base of the nascent primitive streak (Fig. 3O), and throughout the streak during stages 2 and 3 (Fig. 3P). By st. 4, the localization was restricted to the right side of Hensen's node (Fig. 3Q, close-up in Fig. 3R). Sectioning revealed the stain to be mesodermal (Fig. 3S). Polycystin-2 was expressed within the streak from the time of streak elongation (Fig. 3T), with the strongest spot of expression at the base of the streak (Fig. 3U). At st. 4, symmetrical expression was detected in the anterior half of the primitive streak (Fig. 3V). Interestingly, one third (N = 12) of the chick embryos exhibited a right-sided localization of polycystin-2 (Fig. 3W). Sectioning revealed the staining to be localized within the mesoderm cells (Fig. 3X). These data demonstrate that ciliary proteins are present in chick embryos long prior to the formation of Hensen's node and reveal two new asymmetric markers.

Protein Localization Dependence on Cytoskeleton

To gain insight into mechanisms controlling cytoplasmic localization of these proteins (Lutz-Meindl et al., 2003), and begin to assemble an epistatic pathway among the targets, we examined their localization in embryos exposed to reagents that destabilize microtubules (nocodazole: De Brabander et al., 1986; Nuccitelli, 1986; Lane and Keller, 1997) or actin filaments (latrunculin: Ayscough, 1998; Corstens et al., 2003). Because the cytoskeleton is important for mitosis and general cell health, low doses of reagent had to be utilized to permit normal cytokinesis. We reasoned that specific effects on asymmetry could be detected if a dose was found that allowed normal cell division and physiology but disrupted subtle aspects of motor protein function or cytoskeletal organization. We exposed embryos beginning immediately after turning (25 min post-fertilization) to concentrations that permitted cytokinesis and normal subsequent development, and fixed embryos for sectioning and immunohistochemical analysis at the first few cell cleavages. Asymmetric KIF3B localization was, surprisingly, not altered by either treatment (Fig. 4A–C), although latrunculin exposure led to a greater accumulation of signal near the cleavage furrow (Fig. 4C). Polycystin-2 localization to the cell membrane was not altered by nocodazole (Fig. 4D,E) but was disrupted by latrunculin (see Fig. 4F), suggesting that actin elements near the membrane cortex might be necessary for anchoring Polycystin-2 there. Asymmetric localization of acetylated α-tubulin was disrupted by both latrunculin and nocodazole (Fig. 4G, compare to Fig. 4H,I). The rod-like structures reaching for the animal pole characteristic of LRD staining (Fig. 4J) were abolished by targeting either the microtubule or the actin cytoskeleton (Fig. 4K,L), suggesting that both elements of the cytoskeleton are required for the specific rod-like pattern.

The asymmetric localization of Polaris (Fig. 4M) was likewise disrupted by both latrunculin and nocodazole. Interestingly, while treatment with nocodazole (Fig. 4N) uniformly disorganized Polaris localization, Latrunculin exposure resulted in a range of Polaris localization phenotypes, including a more diffuse localization, loss of asymmetry, asymmetry along the presumptive dorso-ventral axis instead of along the LR axis, and central condensation in the cell (Fig. 4O1–O4). The localization of Inversin along the Animal-Vegetal plane includes the rod-like structures reaching animally (Fig. 4P). This specific localization is abolished by nocodazole (Fig. 4Q). Interestingly, Latrunculin exposure led to an increased concentration of Inversin protein in the animal pole throughout the cell and not confined to the normal rod-like structure (Fig. 4R). Strikingly, this occurred asymmetrically, being present in the right side animal pole cells in most of the sections examined (85%, N = 40). The specific membrane localization of Inversin (Fig. 4S) was completely abolished by nocodazole (Fig. 4T).

These observations show that the localization of Polaris, Inversin, LRD, and acetylated α-tubulin are dependent upon subtle and as yet unknown aspects of actin and microtubule cytoskeletal structures.

Dependence of Visceral Asymmetry on Cytoskeleton and Motor Protein Function

To begin to test the hypothesis that early and intracellular functions of the cytoskeleton and/or motor proteins are required for LR patterning, we utilized a loss-of-function approach in *Xenopus*. Because each targeted component has a number of endogenous housekeeping roles, as above we utilized low concentrations of the reagents designed to permit normal development but to target subtle aspects of the cytoskeletal structure that might be required for normal asymmetry. A similar strategy has been previously utilized (with UV-irradiation), showing that it is possible to

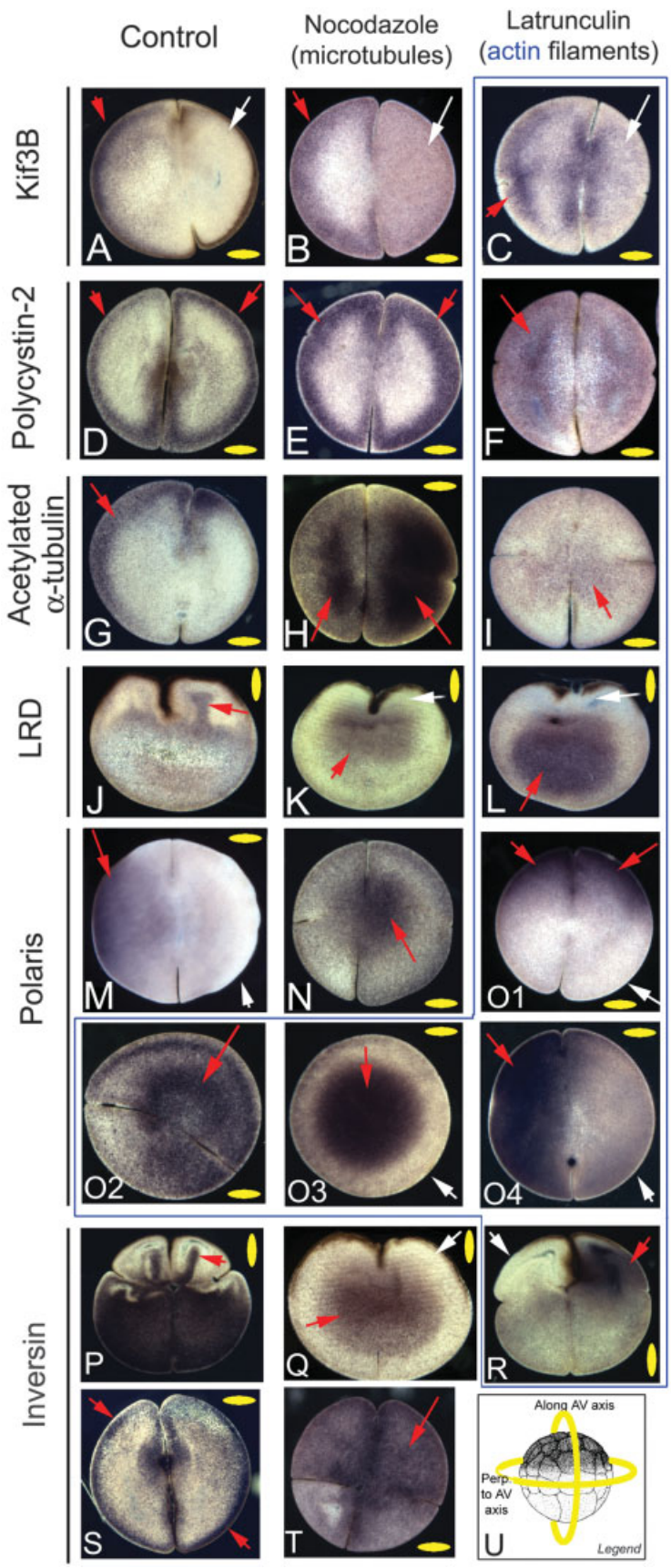

Fig. 4. Dependence of localization patterns on actin and tubulin organization. Microtubules were targeted by nocodazole from fertilization, as described in the Experimental Procedures section. Actin filaments were targeted by latrunculin from fertilization, as described in the Experimental Procedures section. KIF3B: sections taken perpendicular to the AV axis at the 2-cell stage in control embryos (**A**), and those in which microtubules (**B**) or actin filaments (**C**) were targeted. Polycystin-2: sections taken perpendicular to the AV axis at the 2-cell stage in control embryos (**D**), and those in which microtubules (**E**) or actin filaments (**F**) were targeted. Acetylated α-tubulin: sections taken perpendicular to the AV axis at the 4-cell stage in control embryos (**G**), and those in which microtubules (**H**) or actin filaments (**I**) were targeted. LRD: sections taken parallel to the AV axis at the 2-cell stage in control embryos (**J**), and those in which microtubules (**K**) or actin filaments (**L**) were targeted. Polaris: sections taken perpendicular to the AV axis at the 4-cell stage in control embryos (**M**), and those in which microtubules (**N**) or actin filaments (**O1–O4**) were targeted. Inversin: sections taken parallel to the AV axis at the 8-cell stage in control embryos (**P**) or embryos in which microtubules (**Q**) or actin filaments (**R**) were targeted; sections taken perpendicular to the AV axis at the 4-cell stage in control embryos (**S**) and those in which microtubules (**T**) were targeted. **U:** In each panel, yellow ovals with their long axis oriented left to right indicate that the section was taken across the AV axis; yellow ovals with their long axes oriented vertically indicate that the section was taken along the AV axis, with the animal pole being upward. Red arrows, signal; white arrows, lack of signal; green arrows, additional signal.

TABLE 1. Loss-of-Function Data Implicate Cytoplasmic Microtubule-Based Transport in LR Asymmetry[a]

	Control	Dynein antibody	AS2	Microtubules: Nocodazole (st. 1–st. 6)	Microtubules: Nocodazole (st. 6–st. 9)	Actin Filaments (Latrunculin, 1–8 cell)
Situs solitus (w.t.)	100 (100%)	126 (84%)	100 (85%)	59 (81%)	90 (95%)	31 (62%)
Heterotaxic	0 (0%)	24 (**16%**)	18 (**15%**)	14 (**19%**)	5 (**5%**)	19 (38%)
Total	100	150	118	73	95	50
χ^2		15.9	14.6	18.4	3.5	40.1
P value		6.7×10^{-5}	0.0001	1.8×10^{-5}	0.06	2.4×10^{-10}

[a]A blocking anti-dynein antibody or AS2 (inhibitor of kinesin function) as injected into *Xenopus* embryos immediately after fertilization. Nocodazole (a microtubule depolymerization agent) or latrunculin (an actin filament depolymerization agent) was applied in the medium at the stages indicated. Embryos were allowed to develop to st. 45 and scored for the *situs* of the heart, gut, and gall-bladder. The percentage of embryos with one or more of the organs in the reverse orientation (heterotaxia) was analyzed using the χ^2 test with Pearson correction (for increased stringency of the significance test). Boldface indicates the percentage of embryos exhibiting heterotaxia.

dissociate LR- and DV-relevant roles of cortical rotation (Yost, 1991).

To ask whether intracellular motor protein activity was important for normal LR asymmetry, we utilized two loss-of-function reagents: Adociasulfate-2 (AS2), a compound isolated from the marine sponge *Haliclona* that specifically inhibits kinesin activity by targeting its motor domain (Sakowicz et al., 1998), and a function-blocking antibody to the intermediate chain of cytoplasmic dynein, which is not found in flagellar rafts or cilia (Nilsson and Wallin, 1997). Microinjection of AS2 or of the cytoplasmic dynein-blocking antibody into *Xenopus* embryos at the 1-cell stage induced heterotaxia (independent randomization of the positions of the heart, gut apex, and gall bladder) in 15 and 16% of the embryos, respectively (Table 1). Control embryos from the same batch receiving injections of vehicle exhibited the normal (<1%) level of heterotaxia. The effect was statistically significant to $P < 6.7 \times 10^{-5}$ and 0.0001, respectively. We were unable to check specific inhibition of LRD, as our anti-LRD antibody was not function-blocking. While these reagents did not distinguish among the subtypes of dynein and kinesin to determine precisely which are important for LR patterning, the data suggest that *intracellular* functions of kinesin and dynein are required in the LR pathway.

We next sought to examine whether organization of the cytoskeleton was important for LR asymmetry. Exposure of embryos to nocodazole, a blocker of tubulin polymerization, from fertilization to st. 6 (during early cleavage stages) results in 19% of the embryos exhibiting heterotaxia ($P < 1.8 \times 10^{-5}$; Table 1). In contrast, exposure from st. 6 to st. 9^+ (blastula and gastrula stages) induced only 5% heterotaxia. Similarly, exposure to latrunculin from fertilization to the 8-cell stage resulted in 38% heterotaxia ($P < 2.5 \times 10^{-10}$; Table 1). In all cases, the embryos appeared normal (other than laterality randomization) and showed correct (DAI = 5) dorsoanterior development (Danos and Yost, 1996). These results indicate that some aspect of both the microtubule and actin cytoskeleton is required for LR patterning, and, moreover, that this mechanism endogenously functions during cleavage stages (prior to the appearance of the organizer and ciliated cells during gastrulation).

DISCUSSION

Data supporting functional roles for cilia per se in left-right patterning in zebrafish (Amack and Yost, 2004; Essner et al., 2005; Kramer-Zucker et al., 2005) and mouse (Nonaka et al., 2002) indicate that they function during comparatively later stages of development (gastrulation). Genetic mutation experiments that distinguish cytoplasmic roles of motor proteins from ciliary roles, or loss-of-function studies that confine their effect to the pregastrulation embryo, have not been performed. Most importantly, a number of LR patterning mechanisms function prior to the appearance of the mature node in chick and frog embryos, suggesting that nodal cilia are unlikely to be a widely conserved mechanism for the origin of asymmetry, although they may be an intermediate step in the pathway. In the chick, a system of gap-junctional communication (Levin and Mercola, 1999), an asymmetry in membrane voltage (Levin et al., 2002), and a right-sided expression of activin receptor IIa (Stern et al., 1995) occur at early primitive streak stages before the appearance of the node. In the frog, very early (initial cleavage to blastula stage) mechanisms include gap junctional communication (Levin and Mercola, 1998b), ion flux (Levin et al., 2002), the LR coordinator (Hyatt and Yost, 1998), 14-3-3 proteins (Bunney et al., 2003), serotonergic signaling (Fukumoto et al., 2005), and syndecans (Kramer et al., 2002).

While cilia are very good theoretical candidates for an initiator of chirality, no data indicate that they are the first step in asymmetry (as opposed to an important intermediate step in the LR pathway). Indeed, demonstrating that any particular step is itself the origin of asymmetry is difficult, and it is thus necessary to follow known mechanisms backwards. It is particularly important to test early mechanisms in an organism such as *Xenopus*, where the origin of chirality has been pinned down to take place within about 2 hr of time, between fertilization and the second cell cleavage. Because of the

heavy reliance of the early embryo upon maternal proteins during that time, and the potential for post-translational regulation, analysis of mRNA expression is insufficient. Therefore, we directly tested two predictions of the cytoplasmic transport model: that motor proteins and ciliary components would be asymmetrically localized during early embryogenesis within the blastomeres, and that the cytoskeleton is important for this process and for the subsequent LR patterning.

Our immunohistochemistry data relied on a number of antibodies that have mostly been used in mammalian embryos. Two of these have been extensively characterized in the *Xenopus* system and thus are known to be specific for their targets in frog embryos: Kif3B (Le Bot et al., 1998; Ginkel and Wordeman, 2000) and acetylated α-tubulin (Sale et al., 1988; Chu and Klymkowsky, 1989; Dent and Klymkowsky, 1989; LeDizet and Piperno, 1991; Gard et al., 1995a). We characterized two more via Western blotting, and showed that the Polaris antibody and the Polycystin-2 antibody both cleanly recognize targets of the correct predicted size on frog embryo extract (Fig. 1F,G). Thus, data obtained using these four antibodies strongly suggest that we have identified localization patterns of the correct targets.

Three of the other antibodies—LRD, detyrosinated α-tubulin, and Inversin—have not been characterized in frog embryos (in our hands they did not work in Western blots). We commercially generated the LRD antibody to a peptide sequence that was 100% conserved to the vertebrate LRD sequences in the NCBI database. LRD and Inversin antibodies labeled (Fig. 1C,D), as predicted, cilia in older embryos (Bernardini et al., 1999), and a number of different Inversin antibodies give the same staining pattern in early embryos. The ID5 antibody used to detect the detyrosinated α-tubulin is considered to be specific across taxa, and is routinely used in species from *Drosophila* to mammals (Warn et al., 1990; Wheatley et al., 1994; Rudiger et al., 1999; Poole et al., 2001); it has successfully been used to detect detyrosinated tubulin in *Xenopus* cells (Winkelhaus and Hauser, 1997). Thus, it is probable that these antibodies are working correctly in frog embryos. However, it is important to note that in the absence of Western or other data on specificity, we cannot rule out that in frog embryos, the staining pattern we report for these three antibodies includes a component other than that against which the antibodies were designed.

We observed that all of the targets tested were present in the cytoplasm of early *Xenopus* blastomeres. Common to all targets except for Polycystin-2 were symmetrical vegetal localization within the unfertilized egg followed by extremely dynamic patterns within 2 hr after fertilization. Consistent with a role in cytoplasmic aspects of LR patterning, all except for Polycystin-2 exhibited LR differences during the first three cleavages, confirming the existence of LR asymmetries during very early embryogenesis in frog (Levin et al., 2002; Bunney et al., 2003). The immunohistochemistry revealed asymmetric localization patterns, though there was some variability among embryos. Deviations from the reported patterns in a subset of embryos may be due to differences in embryos of slightly-differing age (which would be especially prominent for targets that are dynamically translocated, such as motor proteins), may represent abnormal localization in some embryos that were unhealthy, or may represent endogenous variation within normal parameters.

Asymmetries often included localization to the cell membrane (Fig. 2E,P,V,Af). Membrane localization is unsurprising in the case of Polycystin-2, which is thought to form a cation channel (Vassilev et al., 2001; Koulen et al., 2002) that can be expressed on the cell membrane (Hanaoka et al., 2000) and is transcribed in mouse embryos from the 2-cell stage (Pennekamp et al., 2002). The cell membrane localization of Inversin is perhaps more unexpected, although such a pattern in mammalian embryos has been reported (Eley et al., 2004). These localization data are consistent with non-ciliary roles for inversin in the LR pathway, such as in the modulation of tight-junctions, which are known to be important for LR asymmetry in both chick and frog (Garcia-Castro et al., 2000; Brizuela et al., 2001), and participation in cytoskeletal organization (Eley et al., 2004).

This analysis must be extended in two important ways by future studies. First, movement is impossible to demonstrate in static sections. While our data are consistent with, for example, a dynamic and asymmetric translocation of LRD protein along the LR and AV axes, we are currently attempting to develop a system in which such asymmetric localization can be monitored directly in vivo using fluorescent technology. A related issue is that we can only present here a small subset of images showing sections through what are fairly complex 3-dimensional localizations. Thus, volume reconstruction will probably be necessary to gain a complete understanding of the localization of each target in the large early blastomeres of the frog embryo.

In the chick embryo, all seven of the targets were expressed at the base of the primitive streak during streak initiation and elongation, consistent with models of LR patterning events taking place long before formation of the node. Another commonality was that all were expressed in the mesoderm, suggesting that important LR-patterning events take place in this cell layer. We discovered two consistent asymmetries, identifying LRD and Kif3B as right-sided markers (Fig. 3M,R), although these asymmetries take place during node stages, making them available to participate in LR transport events during late gastrulation as well as possible early roles in the nascent streak. The asymmetry in Kinesin 3B is recapitulated by the recently reported asymmetric localization of the related KIF5-C (Dathe et al., 2004), suggesting that other members of the Kinesin family may be important for asymmetry. Polycystin-2 was right-sided in the node of some embryos, but oddly, it was not consistently asymmetric in all embryos. This may be due to rapid changes in localization as a function of developmental time. While our data characterize the large-scale expression of the target proteins, it will be important in the future to use high-resolution fluorescent microscopy to address subcellular localizations of these proteins in cells at the base of

the primitive streak of the chick embryo.

Our analysis revealed that within the ubiquitous pool of α-tubulin (Fig. 2Ad), there are at least two distinct and asymmetric sub-populations of microtubule proteins, including acetylated (Fig. 2Af) and detyrosinated (Fig. 2Aj) α-tubulin. Although the ID5 antibody reveals a distribution different from the acetylated α-tubulin component, more characterization of this antibody in *Xenopus* will be necessary to show conclusively that it recognizes only the detyrosinated component in frog tissue. While the early frog embryo cytoskeleton has been extensively studied (Gard, 1993, 1994, 1995; Roeder and Gard, 1994; Gard et al., 1995ab–c), most attention has been focused on the oocyte, and subtle LR distributions after cleavage have not heretofore been examined. Interestingly, the localization of a number of the other targets analyzed was dependent on the various elements of the cytoskeleton. For example, the tightly-localized structures revealed as finger-like projections of Inversin and LRD signal are dependent on both the actin and microtubule elements of the cytoskeleton.

Models relying on the early cytoskeleton for orientation of the LR axis (Brown and Wolpert, 1990; Yost, 1991; Levin and Nascone, 1997) predict that transient disruption of such structures should randomize the laterality of the embryo. We observed that exposure to disruptors of the microtubule and the actin cytoskeleton that alters the localization of ciliary proteins indeed induces a specific and significant degree of heterotaxia in the embryos. Laterality was also disrupted by two reagents that specifically target molecular motors. This independent assortment of the heart and viscera took place in the absence of generalized toxicity or midline defects. Most crucially, very early (Table 1) but not later treatment affected asymmetry, supporting our idea that it is the early cytoskeleton-dependent events that are the most salient for embryonic asymmetry.

Our data do not rule out possible later roles of cilia in asymmetry, nor address potential early embryonic function of these proteins in mammalian embryos (although we predict the existence of such). These data also do not suggest an obvious mechanism for what happens in the chick embryo prior to node formation to orient LR asymmetry, beyond suggesting that the initiation of the primitive streak is a good candidate for the LR orientation event (Levin and Mercola, 1998a). Specific molecular models of how this spatial computation is carried out in flat embryos with tens of thousands of small cells must wait for a better understanding of how (and whether) streak cells determine direction along the AP axis (Wei and Mikawa, 2000). However, taken together, our frog data support the following class of models that do not rely on cilia function.

The existence of several ciliary components in the cytoplasm suggests that some of the properties of the ciliary transport complex may be recapitulated inside early blastomeres. Moreover, the concurrence of laterality defects and kidney phenotypes (Mochizuki et al., 1998, 2002; Murcia et al., 2000; Pennekamp et al., 2002; Pazour and Witman, 2003) may reflect similarities in the ways cells utilize subcellular sorting to align their bioelectric potential with their morphological polarization (Alpern, 1996; Al-Awqati et al., 1998; Takito et al., 1999; Vijayakumar et al., 1999). We propose that early asymmetries are generated by the asymmetric shuttling of cargo along oriented cytoskeletal tracks by the molecular motors LRD and Kif3B (Levin, 2003). The ciliary proteins are likely to be either components of the cargo complex (consistent with their mislocalization following exposure to reagents which target the cytoskeleton; Fig. 4) or elements that help to nucleate chiral cytoskeletal structures that direct movement to one direction along the LR axis. The LR-relevant cargo most probably includes mRNA and protein encoding ion transport complexes (Levin et al., 2002; Adams et al., 2005). In addition to H^+ pumps and K^+ channels we have described previously, Polycystin-2 is a candidate, since it controls Ca^{++} flow (Cahalan, 2002) and is regulated by pH and voltage (Gonzalez-Perrett et al., 2002), which is particularly relevant in light of the fact that pH, cell membrane voltage, and Ca^{++} flux have recently been implicated in LR mechanisms not related to cilia function (Levin et al., 2002; Adams and Levin, 2003; Raya et al., 2004).

Consistently with an important early set of experiments indicating that the initial asymmetry in *Xenopus* is generated during the cortical rotation following fertilization (Yost, 1991), the ability to specifically and strongly randomize visceral laterality by reagents that depolymerize microtubules and actin filaments during very early stages (Table 1) showed that the laterality of the embryo was dependent upon the integrity of the early cytoskeleton. By characterizing the roles of myosin, possible chiral structures within the actin cytoskeleton, and the role of the kinesin/dynein families in directing LR-biased localization of ion transporters, we are currently pursuing the asymmetric localization of ion channels and pumps backwards to the origin of left-right asymmetry. An understanding of these events is likely to reveal an exciting and profound consilience of mechanisms allowing subcellular molecular components to align a major body axis during embryogenesis.

EXPERIMENTAL PROCEDURES

Immunohistochemistry

Control, drug-treated, or vehicle-treated frog embryos were fixed in MEMFA overnight at 4°C. They were embedded with care taken to ensure precise orientation with respect to the animal-vegetal axis, sectioned using a Leica Vibratome, and processed for immunohistochemistry using alkaline-phosphatase detection as previously described (Levin, 2004b). Chick embryos were fixed in 4% paraformaldehyde overnight at 4°C, incubated overnight in standard in situ hybridization solution at 70°C to inactivate endogenous alkaline phosphatases, and processed for immunohistochemistry in wholemount using the same protocol as for *Xenopus*. Antibodies were used at the following dilutions for *Xenopus* embryos: KIF3B 1:200 to 1:1,000 (Le Bot et al., 1998; Ginkel and Wordeman, 2000), INV 1:100 to 1:1,000 (Nurnberger et al., 2002), polaris 1:1,000 (Taulman et al., 2001), Polycystin-2 (Pazour et al., 2002) at

1:500 and Santa Cruz no. 10376 at 1:50, ID5 (Wheatley et al., 1994), and acetylated tubulin (Sigma T6793). The LRD antibody was developed commercially for our lab by ResGen as an affinity-purified polyclonal antibody made to a highly conserved peptide in LRD: "SVISIWFEVQRTWSHLES" and used at 1:250 dilution. Concentrations of all antibodies used in chick were generally 4-fold dilutions of those given for *Xenopus*. At least 15 different embryos, with 35 sections from each, were used for each target in *Xenopus*. At least 5 chick embryos were used at each stage for each target.

Embryo Treatment

AS2 stocks were made as 0.4 mg + 50 μL of water. Each 1-cell embryo received injections of a 1:4 dilution of AS2 stock plus rhodamine-linked dextran as a marker. Fifty microliters of dynein antibody (Abcam no. AB6304) were dialyzed against 500 ml of 50 mM potassium glutamate pH 7.2, resuspended in 200 μl K-Glut, and injected directly into 1-cell embryos (standard 2.5-nl injection per cell). Nocodazole and latrunculin (Molecular Probes, Eugene, OR) stocks were made at 5 mg/ml in DMSO. Embryos were treated with nocodazole in the medium at a dilution of 3 μL of stock in 1 L of 0.1X MMR, or with latrunculin in the medium at a dilution of 3 μL of stock in 50 ml of 0.1X MMR. *Xenopus* embryos were staged according to Nieuwkoop and Faber (1967). Chick embryos were staged according to Hamburger and Hamilton (1992).

Western Blotting

Twenty-five *Xenopus* embryos were resuspended in lysis buffer (1% Triton X100, 50 mM NaCl, 10 mM NaF, 1 mM Na_3VO_4, 5 mM EDTA, 10 mM Tris pH 7.6, 2 mM PMSF). Protein solution was mixed at 1:1 with Laemmli sample buffer (Bio-Rad, Richmond, CA) containing 2.5% 2-mercaptoethanol. The proteins were fractionated by SDS-PAGE and electrotransferred to a PVDF membrane. After washing, the membrane was blocked with 3% bovine serum albumin and 5% dry milk in tris-buffered saline including 0.1% Tween-20. It was then incubated overnight in a Mini-PROTEAN II multiscreen apparatus (Bio-Rad) at 4°C with the primary antibody, diluted in TTBS + 3% BSA + 5% dry milk (1:10 for Polaris, 1:20 for Polycystin-2). After washing, the blots were incubated with peroxidase-conjugated second antibody (1:5,000) and developed using an ImmunoStar Chemiluminescent Protein Detection System (Bio-Rad) according to the manufacturer's instructions.

ACKNOWLEDGMENTS

We gratefully thank Linda Wordeman and Isabelle Vernos for antibodies to Kif3B, Bradley Yoder and Greg Pazour for the Polaris antibody, Carrie Phillips for the antibody to Inversin, Vladimir Gelfand for HDkin-5 antibody, Greg Pazour for the Polycystin antibody, Larry Goldstein and Christine Blackburn for AS2, and Debra Sorocco, Adam Crook, and Punita Koustubhan for technical assistance. We also thank Greg Pazour for his comments on an early version of the manuscript and Heather Ward for her kind assistance with INV protein. This investigation was conducted in a Forsyth Institute facility renovated with support from Research Facilities Improvement Grant CO6RR11244 from the National Center for Research Resources, National Institutes of Health.

REFERENCES

Adams DS, Levin M. 2003. Elements of left-right patterning gap junctions, pH, and membrane voltage. Dev Biol 259:482–483.

Adams DS, Robinson KR, Fukumoto T, Yuan S, Yelick P, Kuo L, McSweeney M, Levin M. 2005. The V-ATPase generates asymmetric H+ flux required for correct LR asymmetry in chick and frog embryos. (in press).

Afzelius BA. 1999. Asymmetry of cilia and of mice and men. Int J Dev Biol 43:283–286.

Al-Awqati Q, Vijayakumar S, Hikita C, Chen J, Takito J. 1998. Phenotypic plasticity in the intercalated cell: the hensin pathway. Am J Physiol 275:F183–190.

Alpern RJ. 1996. Hensin: a matrix protein determinant of epithelial polarity. J Clin Invest 98:2189–2190.

Amack JD, Yost HJ. 2004. The T box transcription factor no tail in ciliated cells controls zebrafish left-right asymmetry. Curr Biol 14:685–690.

Arnould T, Sellin L, Benzing T, Tsiokas L, Cohen HT, Kim E, Walz G. 1999. Cellular activation triggered by the autosomal dominant polycystic kidney disease gene product PKD2. Mol Cell Biol 19:3423–3434.

Ayscough K. 1998. Use of latrunculin-A, an actin monomer-binding drug. Methods Enzymol 298:18–25.

Bernardini G, Prati M, Bonetti E, Scarì G. 1999. Atlas of Xenopus development. Milan: Springer.

Brizuela B, Wessely O, DeRobertis E. 2001. Overexpression of the Xenopus tight-junction protein Claudin causes randomization of the left-right body axis. Dev Biol 230:217–229.

Brown N, Wolpert L. 1990. The development of handedness in left/right asymmetry. Development 109:1–9.

Brueckner M. 2001. Cilia propel the embryo in the right direction. Am J Med Genet 101:339–344.

Bunney TD, De Boer AH, Levin M. 2003. Fusicoccin signaling reveals 14-3-3 protein function as a novel step in left-right patterning during amphibian embryogenesis. Development 130:4847–4858.

Burdine R, Schier A. 2000. Conserved and divergent mechanisms in left-right axis formation. Genes Dev 14:763–776.

Cahalan MD. 2002. The ins and outs of polycystin-2 as a calcium release channel. Nature Cell Biol 4:E56–57.

Cai Y, Maeda Y, Cedzich A, Torres VE, Wu G, Hayashi T, Mochizuki T, Park JH, Witzgall R, Somlo S. 1999. Identification and characterization of polycystin-2, the PKD2 gene product. J Biol Chem 274: 28557–28565.

Chu DT, Klymkowsky MW. 1989. The appearance of acetylated alpha-tubulin during early development and cellular differentiation in *Xenopus*. Dev Biol 136: 104–117.

Corstens GJ, Calle M, Roubos EW, Jenks BG. 2003. Role of cortical filamentous actin in the melanotrope cell of *Xenopus laevis*. Gen Comp Endocrinol 134:95–102.

Danos MC, Yost HJ. 1996. Role of notochord in specification of cardiac left-right orientation in zebrafish and Xenopus. Dev Biol 177:96–103.

Dathe V, Prols F, Brand-Saberi B. 2004. Expression of kinesin kif5c during chick development. Anat Embryol (Berl).

De Brabander M, Geuens G, Nuydens R, Willebrords R, Aerts F, De Mey J. 1986. Microtubule dynamics during the cell cycle: the effects of taxol and nocodazole on the microtubule system of Pt K2 cells at different stages of the mitotic cycle. Int Rev Cytol 101:215–274.

Dent JA, Klymkowsky MW. 1989. Whole-mount analysis of cytoskeletal reorganization and function during oogenesis and early embryogenesis in *Xenopus*. In: Shatten H, Shatten G, editors. The cell biology of fertilization. New York: Academic Press. p 63–103.

Eley L, Turnpenny L, Yates LM, Craighead AS, Morgan D, Whistler C, Goodship JA, Strachan T. 2004. A perspective on inversin. Cell Biol Int 28:119–124.

Essner J, Vogan K, Wagner M, Tabin C, Yost H, Brueckner M. 2002. Conserved function for embryonic nodal cilia. Nature 418:37–38.

Essner JJ, Amack JD, Nyholm MK, Harris EB, Yost HJ. 2005. Kupffer's vesicle is a ciliated organ of asymmetry in the zebrafish embryo that initiates left-right development of the brain, heart and gut. Development 132:1247–1260.

Fukumoto T, Kema I, Levin M. 2005. Serotonin signaling is a very early step in patterning of the left-right axis in chick and frog embryos. Curr Biol 15:794–803.

Garcia-Castro M, Vielmetter E, Bronner-Fraser E. 2000. N-cadherin, a cell adhesion molecule involved in establishment of embryonic left-right asymmetry. Science 288:1047–1051.

Gard DL. 1993. Confocal immunofluorescence microscopy of microtubules in amphibian oocytes and eggs. Methods Cell Biol 38:241–264.

Gard DL. 1994. Gamma-tubulin is asymmetrically distributed in the cortex of Xenopus oocytes. Dev Biol 161:131–140.

Gard DL. 1995. Axis formation during amphibian oogenesis: reevaluating the role of the cytoskeleton. Curr Topics Dev Biol 30:215–252.

Gard DL, Affleck D, Error BM. 1995a. Microtubule organization, acetylation, and nucleation in Xenopus laevis oocytes: II. A developmental transition in microtubule organization during early diplotene. Dev Biol 168:189–201.

Gard DL, Cha BJ, Roeder AD. 1995b. F-actin is required for spindle anchoring and rotation in Xenopus oocytes: a re-examination of the effects of cytochalasin B on oocyte maturation. Zygote 3:17–26.

Gard DL, Cha BJ, Schroeder MM. 1995c. Confocal immunofluorescence microscopy of microtubules, microtubule-associated proteins, and microtubule-organizing centers during amphibian oogenesis and early development. Curr Topics Dev Biol 31:383–431.

Ginkel LM, Wordeman L. 2000. Expression and partial characterization of kinesin-related proteins in differentiating and adult skeletal muscle. Mol Biol Cell 11: 4143–4158.

Gonzalez-Perrett S, Batelli M, Kim K, Essafi M, Timpanaro G, Moltabetti N, Reisin IL, Arnaout MA, Cantiello HF. 2002. Voltage dependence and pH regulation of human polycystin-2-mediated cation channel activity. J Biol Chem 277:24959–24966.

Hamburger V, Hamilton H. 1992. A series of normal stages in the development of the chick embryo. Dev Dyn 195:231–272.

Hanaoka K, Qian F, Boletta A, Bhunia AK, Piontek K, Tsiokas L, Sukhatme VP, Guggino WB, Germino GG. 2000. Co-assembly of polycystin-1 and -2 produces unique cation-permeable currents. Nature 408:990–994.

Harrison RE, Huebner E. 1997. Unipolar microtubule array is directly involved in nurse cell-oocyte transport. Cell Motil Cytoskeleton 36:355–362.

Hirokawa N. 2000a. Determination of left-right asymmetry: Role of cilia and KIF3 motor proteins. News Physiol Sci 15:56.

Hirokawa N. 2000b. Stirring up development with the heterotrimeric kinesin KIF3. Traffic 1:29–34.

Hyatt B, Yost H. 1998. The left-right coordinator: the role of Vg1 in organizing left-right axis. Cell 93:37–46.

Koulen P, Cai Y, Geng L, Maeda Y, Nishimura S, Witzgall R, Ehrlich BE, Somlo S. 2002. Polycystin-2 is an intracellular calcium release channel. Nat Cell Biol 4:191–197.

Kramer KL, Barnette JE, Yost HJ. 2002. PKCgamma regulates syndecan-2 inside-out signaling during xenopus left-right development. Cell 111:981–990.

Kramer-Zucker AG, Olale F, Haycraft CJ, Yoder BK, Schier AF, Drummond IA. 2005. Cilia-driven fluid flow in the zebrafish pronephros, brain and Kupffer's vesicle is required for normal organogenesis. Development 132:1907–1921.

Lane MC, Keller R. 1997. Microtubule disruption reveals that Spemann's organizer is subdivided into two domains by the vegetal alignment zone. Development 124:895–906.

Le Bot N, Antony C, White J, Karsenti E, Vernos I. 1998. Role of xklp3, a subunit of the Xenopus kinesin II heterotrimeric complex, in membrane transport between the endoplasmic reticulum and the Golgi apparatus. J Cell Biol 143:1559–1573.

LeDizet M, Piperno G. 1991. Detection of acetylated alpha-tubulin by specific antibodies. Methods Enzymol 196:264–274.

Levin M. 2003. Hypothesis: motor proteins and ion pumps, not ciliary motion, initiate LR asymmetry. BioEssays 25:1002–1010.

Levin M. 2004a. Embryonic origins of left-right asymmetry. Crit Rev Oral Biol Med 15:197–206.

Levin M. 2004b. A novel immunohistochemical method for evaluation of antibody specificity and detection of labile targets in biological tissue. J Biochem Biophys Methods 58:85–96.

Levin M. 2005. Left-right asymmetry in embryonic development: a comprehensive review. Mech Dev 122:3–25.

Levin M, Mercola M. 1998a. The compulsion of chirality: toward an understanding of left- right asymmetry. Genes Dev 12:763–769.

Levin M, Mercola M. 1998b. Gap junctions are involved in the early generation of left right asymmetry. Dev Biol 203:90–105.

Levin M, Mercola M. 1999. Gap junction-mediated transfer of left-right patterning signals in the early chick blastoderm is upstream of Shh asymmetry in the node. Development 126:4703–4714.

Levin M, Nascone N. 1997. Two molecular models of initial left-right asymmetry generation. Med Hypotheses 49:429–435.

Levin M, Thorlin T, Robinson KR, Nogi T, Mercola M. 2002. Asymmetries in H+/K+-ATPase and cell membrane potentials comprise a very early step in left-right patterning. Cell 111:77–89.

Lowe LA, Supp DM, Sampath K, Yokoyama T, Wright CV, Potter SS, Overbeek P, Kuehn MR. 1996. Conserved left-right asymmetry of nodal expression and alterations in murine situs inversus. Nature 381:158–161.

Lutz-Meindl AH. 2003. Evidence for kinesin- and dynein-like protein function in circular nuclear migration in the green alga Pleurenterium tumidum: digital time lapse analysis of inhibitor effects. J Phycol 39:106–114.

Maruta H, Greer K, Rosenbaum JL. 1986. The acetylation of alpha-tubulin and its relationship to the assembly and disassembly of microtubules. J Cell Biol 103: 571–579.

McGrath J, Brueckner M. 2003. Cilia are at the heart of vertebrate left-right asymmetry. Curr Opin Genet Dev 13: 385–392.

Mochizuki T, Saijoh Y, Tsuchiya K, Shirayoshi Y, Takai S, Taya C, Yonekawa H, Yamada K, Nihei H, Nakatsuji N, Overbeek P, Hamada H, Yokoyama T. 1998. Cloning of inv, a gene that controls left/right asymmetry and kidney development. Nature 395:177–181.

Mochizuki T, Tsuchiya K, Yokoyama T. 2002. Molecular cloning of a gene for inversion of embryo turning (inv) with cystic kidney. Nephrol Dial Transplant 17: 68–70.

Morales M, Fifkova E. 1991. Distribution of acetylated alpha-tubulin in brain. In situ localization and biochemical characterization. Cell Tissue Res 265:415–423.

Morgan D, Turnpenny L, Goodship J, Dai W, Majumder K, Matthews L, Gardner A, Schuster G, Vien L, Harrison W, Elder FF, Penman-Splitt M, Overbeek P, Strachan T. 1998. Inversin, a novel gene in the vertebrate left-right axis pathway, is partially deleted in the inv mouse. Nature Genet 20:149–156.

Morgan D, Goodship J, Essner JJ, Vogan KJ, Turnpenny L, Yost HJ, Tabin CJ, Strachan T. 2002. The left-right determinant inversin has highly conserved ankyrin repeat and IQ domains and interacts with calmodulin. Human Genet 110:377–384.

Murcia NS, Richards WG, Yoder BK, Mucenski ML, Dunlap JR, Woychik RP. 2000. The Oak Ridge Polycystic Kidney (orpk) disease gene is required for left-right axis determination. Development 127:2347–2355.

Nieuwkoop PD, Faber J. 1967. Normal Table of *Xenopus laevis* (Daudin). Amsterdam: North-Holland Publishing Company.

Nilsson H, Wallin M. 1997. Evidence for several roles of dynein in pigment transport in melanophores. Cell Motil Cytoskeleton 38:397–409.

Nilsson H, Rutberg M, Wallin M. 1996. Localization of kinesin and cytoplasmic dynein in cultured melanophores from Atlantic cod, *Gadus morhua*. Cell Motil Cytoskeleton 33:183–196.

Nonaka S, Tanaka Y, Okada Y, Takeda S, Harada A, Kanai Y, Kido M, Hirokawa N. 1998. Randomization of left-right asymmetry due to loss of nodal cilia generating leftward flow of extraembryonic fluid in mice lacking KIF3B motor protein. Cell 95:829–837.

Nonaka S, Shiratori H, Saijoh H, Hamada H. 2002. Determination of left-right patterning of the mouse embryo by artificial nodal flow. Nature 418:96–99.

Nuccitelli R. 1986. A two-dimensional extracellular vibrating probe for the detection of trans-cellular ionic currents. J Cell Biol 103:A519–A519.

Nurnberger J, Bacallao RL, Phillips CL. 2002. Inversin forms a complex with catenins and N-cadherin in polarized epithelial cells. Mol Biol Cell 13:3096–3106.

Nurnberger J, Kribben A, Saez AO, Heusch G, Philipp T, Phillips CL. 2004. The Invs gene encodes a microtubule-associated protein. J Am Soc Nephrol 15: 1700–1710.

Pazour GJ, Witman GB. 2003. The vertebrate primary cilium is a sensory organelle. Curr Opin Cell Biol 15:105–110.

Pazour GJ, Dickert BL, Vucica Y, Seeley ES, Rosenbaum JL, Witman GB, Cole DG. 2000. Chlamydomonas IFT88 and its mouse homologue, polycystic kidney disease gene tg737, are required for assembly of cilia and flagella. J Cell Biol 151:709–718.

Pazour GJ, San Agustin JT, Follit JA, Rosenbaum JL, Witman GB. 2002. Polycystin-2 localizes to kidney cilia and the ciliary level is elevated in orpk mice with polycystic kidney disease. Curr Biol 12: R378–380.

Pennekamp P, Karcher C, Fischer A, Schweickert A, Skryabin B, Horst J, Blum M, Dworniczak B. 2002. The ion channel polycystin-2 is required for left-right axis determination in mice. Curr Biol 12:938–943.

Poole CA, Zhang ZJ, Ross JM. 2001. The differential distribution of acetylated and detyrosinated alpha-tubulin in the microtubular cytoskeleton and primary cilia of hyaline cartilage chondrocytes. J Anat 199:393–405.

Raya A, Kawakami Y, Rodriguez-Esteban C, Ibanes M, Rasskin-Gutman D, Rodriguez-Leon J, Buscher D, Feijo JA, Izpisua Belmonte JC. 2004. Notch activity acts as a sensor for extracellular calcium during vertebrate left-right determination. Nature 427:121–128.

Rodionov VI, Gyoeva FK, Gelfand VI. 1991. Kinesin is responsible for centrifugal movement of pigment granules in melanophores. Proc Natl Acad Sci USA 88: 4956–4960.

Roeder AD, Gard DL. 1994. Confocal microscopy of F-actin distribution in Xenopus oocytes. Zygote 2:111–124.

Rudiger AH, Rudiger M, Wehland J, Weber K. 1999. Monoclonal antibody ID5: epitope characterization and minimal requirements for the recognition of polyglutamylated alpha- and beta-tubulin. Eur J Cell Biol 78:15–20.

Sakowicz R, Berdelis MS, Ray K, Blackburn CL, Hopmann C, Faulkner DJ, Goldstein LS. 1998. A marine natural product inhibitor of kinesin motors. Science 280:292–295.

Sale WS, Besharse JC, Piperno G. 1988. Distribution of acetylated alpha-tubulin in retina and in vitro-assembled microtubules. Cell Motil Cytoskeleton 9:243–253.

Stern C, Yu R, Kakizuka A, Kintner C, Mathews L, Vale W, Evans R, Umesono K. 1995. Activin and its receptors during gastrulation and the later phases of mesoderm development in the chick embryo. Dev Biol 172:192–205.

Supp DM, Witte DP, Potter SS, Brueckner M. 1997. Mutation of an axonemal dynein affects left-right asymmetry in inversus viscerum mice. Nature 389:963–966.

Supp DM, Brueckner M, Kuehn M, Witte D, Lowe L, McGrath J, Cirrakes J, Potter S. 1999a. Targeted deletion of the ATP binding domain of left-right dynein confirms its role in specifying development of left-right asymmetries. Development 126:5495–5504.

Supp DM, Brueckner M, Kuehn MR, Witte DP, Lowe LA, McGrath J, Corrales J, Potter SS. 1999b. Targeted deletion of the ATP binding domain of left-right dynein confirms its role in specifying development of left-right asymmetries. Development (Suppl) 126:5495–5504.

Tabin CJ, Vogan KJ. 2003. A two-cilia model for vertebrate left-right axis specification. Genes Dev 17:1–6.

Takeda S, Yonekawa Y, Tanaka Y, Okada Y, Nonaka S, Hirokawa N. 1999. Left-right asymmetry and kinesin superfamily protein KIF3A: new insights in determination of laterality and mesoderm induction by kif3A-/- mice analysis. J Cell Biol 145:825–836.

Takito J, Yan L, Ma J, Hikita C, Vijayakumar S, Warburton D, Al-Awqati Q. 1999. Hensin, the polarity reversal protein, is encoded by DMBT1, a gene frequently deleted in malignant gliomas. Am J Physiol 277:F277–289.

Taulman PD, Haycraft CJ, Balkovetz DF, Yoder BK. 2001. Polaris, a protein involved in left-right axis patterning, localizes to basal bodies and cilia. Mol Biol Cell 12:589–599.

Vassilev PM, Guo L, Chen XZ, Segal Y, Peng JB, Basora N, Babakhanlou H, Cruger G, Kanazirska M, Ye C, Brown EM, Hediger MA, Zhou J. 2001. Polycystin-2 is a novel cation channel implicated in defective intracellular Ca(2+) homeostasis in polycystic kidney disease. Biochem Biophys Res Commun 282:341–350.

Vijayakumar S, Takito J, Hikita C, Al-Awqati Q. 1999. Hensin remodels the apical cytoskeleton and induces columnarization of intercalated epithelial cells: processes that resemble terminal differentiation. J Cell Biol 144:1057–1067.

Vogan KJ, Tabin CJ. 1999. A new spin on handed asymmetry. Nature 397:295, 297–298.

Warn RM, Harrison A, Planques V, Robert-Nicoud N, Wehland J. 1990. Distribution of microtubules containing post-translationally modified alpha-tubulin during Drosophila embryogenesis. Cell Motil Cytoskeleton 17:34–45.

Webster DR, Wehland J, Weber K, Borisy GG. 1990. Detyrosination of alpha tubulin does not stabilize microtubules in vivo. J Cell Biol 111:113–122.

Wei Y, Mikawa T. 2000. Formation of the avian primitive streak from spatially restricted blastoderm: evidence for polarized cell division in the elongating streak. Development 127:87–96.

Wheatley DN, Feilen EM, Yin Z, Wheatley SP. 1994. Primary cilia in cultured mammalian cells: detection with an antibody against detyrosinated alpha-tubulin (ID5) and by electron microscopy. J Submicrosc Cytol Pathol 26:91–102.

Winkelhaus S, Hauser M. 1997. Orthovanadate affects both the tyrosination/detyrosination state of spindle microtubules and the organization of XTH-2 spindles. Eur J Cell Biol 73:306–315.

Yokoyama T, Copeland NG, Jenkins NG, Montgomery CA, Elder FF, Overbeek PA. 1993. Reversal of left-right asymmetry: a situs inversus mutation. Science 260:679–682.

Yost HJ. 1991. Development of the left-right axis in amphibians. Ciba Found Symp 162:165–176.

Yost HJ. 2001. Establishment of left-right asymmetry. Int Rev Cytol 203:357–381.